Journal of Mathematical Chemistry 10(1992)205–220

AN ENERGY DECOMPOSITION ANALYSIS OF INTERMOLECULAR INTERACTIONS

Inge RØEGGEN
Institute of Mathematical and Physical Sciences, University of Tromsø, 9000 Tromsø, Norway

Abstract

Within the context of extended geminal models the concepts of charge centroids and charge ellipsoids of the geminal one-electron densities, and an energy decomposition of the intermolecular potential, are introduced as tools of analysis. The intermolecular potential can within this framework be written as a sum of the distortion energies of the subsystems and the interaction energies between the distorted subsystems. The interaction energy is further partitioned into a Coulombic, exchange and correlation contribution. Three classes of complexes are studied: hydrogen bonded systems $(HF)_2$, H_2OHF, $(H_2O)_2$; strongly bonded electron donor–acceptor (EDA) complexes: BH_3NH_3, BH_3CO; and weakly bonded EDA complexes: F_2NH_3, Cl_2NH_3 and $ClFNH_3$. The main results of the calculations, using basis sets consisting of [9s, 6p, 2d] (Cl), [7s, 4p, 2d] (B, N, O, F), [4s, 2p] (H) contracted Gaussian-type functions, and the numerical models EXRHF3 and EXGEM7, are as follows. The bonding in these complexes is essentially due to a lone pair of the donor subsystems approaching the "vacant" space in the vicinity of a nucleus of the acceptor system. The interaction energy is therefore dominated by the Coulombic term. However, the sum of the distortion terms is larger than the magnitude of the Coulombic term. Hence, the exchange and correlation terms give a substantial contribution to the intermolecular potential. If the components of the decomposition of the potential are rescaled by using the magnitude of the interaction energy as the energy unit, a remarkable similarity between the three classes of complexes is disclosed.

1. Introduction

The intermolecular potential is a key concept in chemical physics. It is of paramount importance for such diverse phenomena as gas imperfections, molecular scattering cross sections, transport properties of gases, and the properties of the liquid and the solid state.

There are two main theoretical problems related to the intermolecular potential. The first problem is a computational one. In order to obtain accurate potentials, one needs large basis sets and a computational model which yields a balanced description of the intrasystem correlation energy. The second problem is an interpretative one. There is a need for concepts which help to elucidate the physical origin of the interaction. Furthermore, the constructed concepts should also serve as tools for discovering similarities and differences among Van der Waals systems.

There are two main classes for the calculation of intermolecular potentials: methods which are based on considering the interaction between the subsystems as a perturbation and supermolecule methods considering the interacting subsystems as a supermolecule. A description of these different approaches and with reference to the literature may be found in the monographs by Maitland et al. [1] and Hobza and Zahradnik [2]. Within the supermolecule class Røeggen [3–9] has introduced a novel approach both for computation and analysis of intermolecular interactions. This approach is formulated within the framework of extended geminal models. These models are size extensive, they can be applied for any intersystem distance, and they have a conceptual structure which facilitates interpretation. For these models, there is a very simple energy decomposition scheme. The total electronic energy of the supersystem can be written as a sum of intra- and intersystem energies. As a consequence of this partitioning, the intermolecular potential is obtained as a sum of intrasystem distortion energies and intersystem energies. The intersystem energies can be further partitioned into Coulombic, exchange and correlation components.

The purpose of the present work is to use the energy decomposition analysis to illuminate the differences and similarities between three classes of Van der Waals complexes: hydrogen bonded systems: $(HF)_2$, H_2OHF, $(H_2O)_2$; strongly bonded electron donor–acceptor (EDA) complexes: BH_3NH_3, BH_3CO; and weakly bonded EDA complexes: F_2NH_3, Cl_2NH_3 and $ClFNH_3$.

The structure of the paper is as follows. In section 2 we give a brief account of the theoretical framework. Section 3 is devoted to computational details. In section 4 we present the results for the selected systems.

2. The theoretical framework

In refs. [4,5,9] we have given a detailed description of the theoretical approach adopted in this work. Accordingly, in this section we sketch only the essential elements of the theory needed to make our work readable.

2.1. EXTENDED GEMINAL MODELS

If the general extended geminal model [3] is truncated at the double-pair correction level, we have the following ansatz for the electronic wave function of a closed shell $2N$-electron system:

$$\Phi^{EXG} = \Phi^{APSG} + \sum_{K=1}^{N} \Psi_K + \sum_{K<L}^{N} \Psi_{KL}. \tag{1}$$

In eq. (1), Φ^{APSG} denotes the APSG function, i.e. the antisymmetric product of strongly orthogonal geminals, Ψ_K represents a single pair correction term, and Ψ_{KL} a double pair correction term. The energy can be formally evaluated within the framework of the method of moments. Since, by construction, we have

$$\langle \Phi^{\mathrm{APSG}} | \Phi^{\mathrm{EXG}} \rangle = 1, \tag{2}$$

it follows that

$$\begin{aligned} E^{EXG} &= \langle \Phi^{\mathrm{APSG}} | H \Phi^{\mathrm{ECG}} \rangle \\ &= E^{\mathrm{APSG}} + \sum_{K=1}^{N} \varepsilon_K + \sum_{K<L}^{N} \varepsilon_{KL}, \end{aligned} \tag{3}$$

where

$$E^{\mathrm{APSG}} = \langle \Phi^{\mathrm{APSG}} | H \Phi^{\mathrm{APSG}} \rangle, \tag{4}$$

$$\begin{aligned} \varepsilon_K &= \langle \Phi^{\mathrm{APSG}} | H \Psi_K \rangle \\ &= \langle \Lambda_K | H^K_{\mathrm{eff}} \Omega^{[2]}_K \rangle, \end{aligned} \tag{5}$$

$$\begin{aligned} \varepsilon_{KL} &= \langle \Phi^{\mathrm{APSG}} | H \Psi_{KL} \rangle \\ &= \langle \Phi^{\mathrm{APSG}}_{KL} | H^{KL}_{\mathrm{eff}} \Omega^{[4]}_{KL} \rangle. \end{aligned} \tag{6}$$

In eq. (5) H^K_{eff} is an effective two-electron Hamiltonian for electron pair K [5] and H^{KL}_{eff} in eq. (6) is an effective Hamiltonian for the four-electron cluster defined by electron pairs K and L. Furthermore, Λ_K is the APSG geminal for electron pair K and $\Phi^{\mathrm{APSG}}_{KL}$ is the APSG function for the four-electron system (K, L).

The difficult problem within this framework is to calculate the double pair correction term $\{\varepsilon_{KL}\}$. Previously, we have introduced different approximations [6, 8] for these terms, leading to different numerical models. The most sophisticated ones are the EXGEM7 and EXRHF3 models [8], which shall be adopted in this work. In the EXGEM7 model, there is at least one geminal Λ_K which is described by more than one natural orbital. Geminals described by only one natural orbit, i.e. restricted Hartree–Fock (RHF) geminals, are localized by minimizing the Coulomb repulsion between the corresponding electron pairs. When all geminals $\{\Lambda_K\}$ are RHF-geminals, the corresponding model is denoted the EXRHF3 model.

2.2. LOCALIZATION MEASURES OF THE GEMINAL ONE-ELECTRON DENSITIES

A commonly adopted way of describing the localization of the geminals is by means of charge centroids. The charge centroids are a set of vectors which are defined on the basis of the expression for the electronic part of the electric dipole moment. A straightforward derivation leads to the following well-known relation:

$$\langle \Phi^{\mathrm{APSG}} | -\sum_{i=1}^{2N} r_i | \Phi^{\mathrm{APSG}} \rangle = -\sum_{K=1}^{N} \int P_1^K(\boldsymbol{r}) \boldsymbol{r} \, \mathrm{d}\upsilon$$

$$= -\sum_{K=1}^{N} 2 \int \tfrac{1}{2} P_1^K(\boldsymbol{r}) \boldsymbol{r} \, \mathrm{d}\upsilon = -\sum_{K=1}^{N} 2\boldsymbol{r}^K, \tag{7}$$

where $\boldsymbol{r}^K$ is the average position, or charge centroid, of the two electrons associated with the geminal Λ_K.

Following Robb et al. [10] and Csizmadia [11], we define a measure of the extension of the geminal one-electron density, by means of the seond-order moments of the position operator, using the charge centroid as a local origin. The second-order moments (or variance matrix) are defined by the relations

$$M_{rs} = \tfrac{1}{2} \int \left[\left(x_r' - x_r^K \right) \left(x_s' - x_s^K \right) \right] P_1^K(\boldsymbol{r}') \mathrm{d}\upsilon', \quad r,s \in \{1, 2, 3\}, \tag{8}$$

where x_r^K is the rth component of the charge centroid $\boldsymbol{r}^K$ defined in eq. (7) and P_1^K is the one-electron density associated with the geminal Λ_K. The factor 1/2 in front of the integral is due to the fact that we have equal contributions to the spatial density from electrons with α- and β-spin. If we diagonalize this symmetric variance matrix, we obtain what we may denote as a charge ellipsoid. The eigenvalues $\{a_1, a_2, a_3\}$ of the matrix (M_{rs}) correspond to the squares of the half-axes of the ellipsoid. The standard deviations in three orthogonal directions are therefore given by

$$\Delta l_i = \sqrt{a_i}, \quad i \in \{1,2,3\}. \tag{9}$$

The quantities $\{\Delta l_i\}$ can then be used as a measure of the extension of the geminal one-electron density. Furthermore, we may also use the volume of the ellipsoid as a single number of the extension of the geminal one-electron density:

$$V = \frac{4\pi}{3} \Delta l_1 \Delta l_2 \Delta l_3 . \tag{10}$$

2.3. PARTITIONING OF THE TOTAL ELECTRONIC ENERGY AND THE INTERMOLECULAR POTENTIAL

By using the localization measures introduced in subsection 2.2, a molecular system can be partitioned into fragments or subsystems. Electron pairs and nuclei localized in the same part of the physical space define the fragments (see figs. 3–10).

In some recent works, Røeggen [4] and Røeggen and Wisløff-Nilssen [5] have shown that the total electronic energy, i.e. the total energy in the absence of nuclear motion, can, within the framework of extended geminal models, be written as a sum of intra- and interfragment energies:

$$E^{\mathrm{EXG}}_{\mathrm{supersystem}} \equiv E^{\mathrm{EXG}} + E_{\mathrm{nuc}}$$

$$= \sum_{\gamma} E^{\mathrm{frag},\gamma} + \sum_{\gamma<\delta} E^{\mathrm{frag},\gamma-\mathrm{frag},\delta}. \tag{11}$$

In eq. (11), E_{nuc} denotes the nuclear electrostatic energy, and the summations run over the fragments or the distinct pairs of fragments. The key element in deriving eq. (11) was the partitioning of the one-electron potential according to the formula

$$V(1) = \sum_{\gamma} V^{\mathrm{frag},\gamma}(1). \tag{12}$$

When there are no nuclei in fragment γ, $V^{\mathrm{frag},\gamma}$ is the zero operator. Otherwise,

$$V^{\mathrm{frag},\gamma}(1) = -\sum_{\alpha} \frac{Z_\alpha}{r_{\alpha,1}}. \tag{13}$$

In eq. (13), the summation runs over the number of nuclei in the fragment and Z_α is the nuclear charge (in atomic units) of nucleus α. The partitioning is then simply obtained by grouping the terms associated with each fragment and each pair of fragments.

The intrafragment energy can be partitioned into a kinetic, Coulombic, exchange and correlation contribution:

$$E^{\mathrm{frag},\gamma} = E^{\mathrm{frag},\gamma}_{\mathrm{kin}} + E^{\mathrm{frag},\gamma}_{\mathrm{coul}} + E^{\mathrm{frag},\gamma}_{\mathrm{exch}} + E^{\mathrm{frag},\gamma}_{\mathrm{corr}}. \tag{14}$$

A straightforward partitioning of the interfragment energy yields

$$E^{\mathrm{frag},\gamma-\mathrm{frag},\delta} = E^{\mathrm{frag},\gamma-\mathrm{frag},\delta}_{\mathrm{coul}} + E^{\mathrm{frag},\gamma-\mathrm{frag},\delta}_{\mathrm{exch}} + E^{\mathrm{frag},\gamma-\mathrm{frag},\delta}_{\mathrm{corr}}, \tag{15}$$

where the three components represent the Coulombic, exchange and correlation contribution to the interaction energy, respectively.

As for the intermolecular potential U, we obtain a conceptually and physically very simple decomposition:

$$U = E^{\mathrm{EXG}}_{\mathrm{supersystem}} - \sum_{\gamma} E^{\mathrm{frag},\gamma}_{\mathrm{isolated}}$$

$$= \sum_{\gamma} \left\{ E^{\mathrm{frag},\gamma}_{\mathrm{supersystem}} - E^{\mathrm{frag},\gamma}_{\mathrm{isolated}} \right\} + \sum_{\gamma<\delta} E^{\mathrm{frag},\gamma-\mathrm{frag},\delta}$$

$$= \Delta_{\mathrm{dist}} + \Delta_{\mathrm{int}}$$

$$= \sum_{\gamma} \Delta^{\gamma}_{\mathrm{dist}} + \sum_{\gamma<\delta} \left\{ \Delta^{\gamma,\delta}_{\mathrm{coul}} + \Delta^{\gamma,\delta}_{\mathrm{exch}} + \Delta^{\gamma,\delta}_{\mathrm{corr}} \right\}. \tag{16}$$

In the last equation, $\Delta_{\text{dist}}^{\gamma}$ is the distortion energy of the subsystem γ due to the presence of the other subsystems. The interaction energy Δ_{int} is simply the sum of the Coulombic, exchange and correlation part in eq. (16).

In the terminology we are using in this work, there is a clear distinction between the intermolecular potential and the interaction energy between the subsystems. The intermolecular potential U is defined by the Born–Oppenheimer approximation. It is the effective potential that governs the motion of the *nuclei*. The interaction energy between the subsystems is the interaction energy between the subsystems including both *nuclei* and *electrons*. As expressed by eq. (16), the intermolecular potential can be expressed in terms of the distortion energies and the interaction energies between the subsystems.

2.4. REDUCTION OF THE BSSE

In correcting for the basis set superposition error (BSSE), we follow the procedure described in ref. [9]. The correction scheme is as follows. As for the intrapair correction $\{\varepsilon_K\}$, we use exactly the same number of natural orbitals (NOs) in describing the improved geminal $(\Lambda_K + \Omega_K^{[2]})$ in both the isolated subsystem and the subsystem in the supermolecule. Since the geminal one-electron density P_1^K (defined by Λ_K) is localized in a restricted part of the physical space, the correlating orbitals defining $\Omega_K^{[2]}$ will also be localized in the same part of the physical spcae. Moreover, since in both cases the forms of the correlating orbitals are determined by the optimization procedure, the orbital space associated with $\Omega_K^{[2]}$ will be almost identical in these two cases. The intrafragment double pair correction terms $\{\varepsilon_{LK}\}$ could in principle be treated in an analogous way. However, numerical experience indicates that the actual changes in the double pair correction terms overestimate the changes taking place during dimer formation. For the time being, we therefore neglect the changes in intrasystem double pair correction terms. In future work, we shall eliminate this weakness of our models, as outlined in ref. [9].

3. Computational details

The basis sets used in this study are constructed in the following way. For the chlorine atoms, we start with Huzinaga's (12s, 9p) uncontracted Gaussian-type functions [12] contracted to (7s, 5p] using contraction coefficients from atomic SCF calculations. The contracted set is augmented by two diffuse s-type functions and one set of diffuse p-type functions. The exponents of the diffuse functions are determined as an even-tempered extension of the original set. We add two sets of polarization functions. The first is appropriate for describing intra-atomic correlation (exponents 0.68 [13]), and the second is suitable for describing dispersion-type interactions (exponents 0.15 [14]). The final basis set for the chlorine atoms is then [9s, 6p, 2d]. The basis sets used for the first row atoms (B, C, O, F) are [7s, 4p, 2d]

contracted Gaussian-type functions [9,15], and the hydrogen atoms are described by a [4s, 2p] set [9].

In all calculations, we are using the Beebe–Linderberg two-electron integral approximation [16,17]. We select an integral threshold of $\delta = 10^{-7}$ a.u. Test calculations on the HF molecule demonstrate that by using this integral threshold, the errors in the calculated energy should be less than 10^{-6} a.u. [17].

From a conceptual point of view, we should use the EXGEM model rather than the EXRHF model. Proper geminals, i.e. geminals with $n_K > 1$, are uniquely defined and no localization is needed. However, the calculation of an APSG function is computationally far more demanding than solving the standard RHF equations. Accordingly, the EXGEM model is only used when the RHF function yields a poor description of the bonding in the monomers.

It is well-known that an RHF description of the CO molecule yields the wrong sign of the electric dipole moment. An APSG function can eliminate this deficiency. By using two natural orbitals for each of the bond pair geminals, the RHF geminals for core electron pairs and lone pairs, we obtain an electric dipole moment with the correct polarity, i.e. $C^{-\delta}O^{+\delta}$. For the calculated equilibrium distance, the dipole moment is 0.1356 Debye.

The bond pair geminals in F_2, Cl_2 and ClF are described by two natural orbitals, while the molecules BH_3, NH_3, HF and H_2O are described by only RHF geminals in the root function.

According to the procedure defined in subsection 2.4, we use the same number of NOs in describing the improved geminal $(\Lambda_K + \Omega_K^{[2]})$ in both the isolated subsystem and the subsystem in the supersystem. We choose a maximum of 51 NOs for all subsystems involved. In the supersystem calculation, we use second-order perturbation theory to calculate an approximate correction term $\tilde{\Omega}_K^{[2]}$. This correction term is based on the full common orbital space for the supersystem. We then express $\tilde{\Omega}_K^{[2]}$ in terms of NOs, and pick out the selected number of NOs with the highest occupation numbers. This set of NOs is the subspace of the full common orbital space defining $\tilde{\Omega}_K^{[2]}$.

All *intersystem* double pair correction terms $\{\varepsilon_{KL}^{(2)}\}$ are defined in terms of 52 dispersion-type NOs [7,8]. The full CI corrections $\{\varepsilon_{KL}^{(3)}\}$ are calculated in an orbital subspace consisting of 26 NOs. The full CI corrections correspond to only approximately 1% of the total intersystem correlation energy for the hydrogen bonded systems, and they are therefore neglected for that particular class of Van der Waals complexes. On the other hand, these terms yield 29.7% of the intersystem correlation energy for BH_3NH_3.

4. Results

In this work, we shall put forward the conjecture that the bonding in a large group of Van der Waals complexes is essentially due to an electron pair of one subsystem approaching the "vacant" space around the nucleus of another subsystem.

This point of view shall be supported by looking at the spatial extension of the geminal one-electron densities of the subsystems, and an energy decomposition analysis emphasizing the Coulombic interaction between the distorted subsystems.

Throughout this work, we shall use a terminology implying that the donor subsystem is the one supplying the electron pair which is approaching a nucleus of the acceptor subsystem.

Three groups of dimers are studied:

(i) Strongly bonded EDA-complexes: BH_3CO and BH_3NH_3.

(ii) Weakly bonded EDA-complexes: F_2NH_3, Cl_2NH_3 and $ClFNH_3$.

(iii) Hydrogen bonded systems: $(HF)_2$, H_2OHF and $(H_2O)_2$.

4.1. STRUCTURE

The procedure for obtaining the equilibrium geometry of the dimers is the following. The geometry of the isolated subsystems is optimized at the EXRHF3 or EXGEM7 level of theory. For all subsystems except BH_3, the geometry of the subsystems in the dimers is fixed and equal to the geometry of the isolated monomers. For the subsystem BH_3 in the two dimers in question, we use the same bond length as in the optimized planar BH_3, but the bond angle HBH is chosen equal to the value determined by Breulet et al. [18]. The only parameters which are optimized for the dimers are the dimer distance for the strong and weakly bonded EDA complexes, and the dimer distance and two angles for the hydrogen bonded systems. The equilibrium structures of the eight complexes studied in this work are displayed in figs. 1 and 2.

In fig. 3, we display the electronic structure of the dimer BH_3CO in terms of charge ellipsoids and charge centroids of selected geminals. This figure clearly indicates that the origin of the bonding subsystems is due to the lone pair of carbon approaching the "vacant" space in the vicinity of the boron nucleus. The charge centroid of the carbon lone pair is shifted 0.26231 a.u. away from the carbon nucleus and towards the boron nucleus. There are smaller shifts of the oxygen lone pair and σ-type bond pair centroids towards the boron nucleus. As for the π-type bond pair geminal, each of the GVB-type charge centroids is shifted towards the atomic nucleus they are associated with. The electric dipole moment of the CO subsystem changes from 0.0528 a.u. to 0.7090 a.u. during formation of the complex. The changes of the bond pair geminals of BH_3 are slightly more subtle. The bond pair ellipsoids are bent backwards during dimerization, leaving more available space for the approaching carbon lone pair, the charge centroids of the bond pairs are slightly shifted towards the boron nucleus, and the corresponding charge ellipsoids expand along all three half-axes. The electric dipole moment of the borane subsystem changes from 0.0 a.u. to 0.2530 a.u.

In fig. 4, we display the intersection between the xy-plane and the selected charge centroids of borazane. This figure makes the origin of the bonding of the

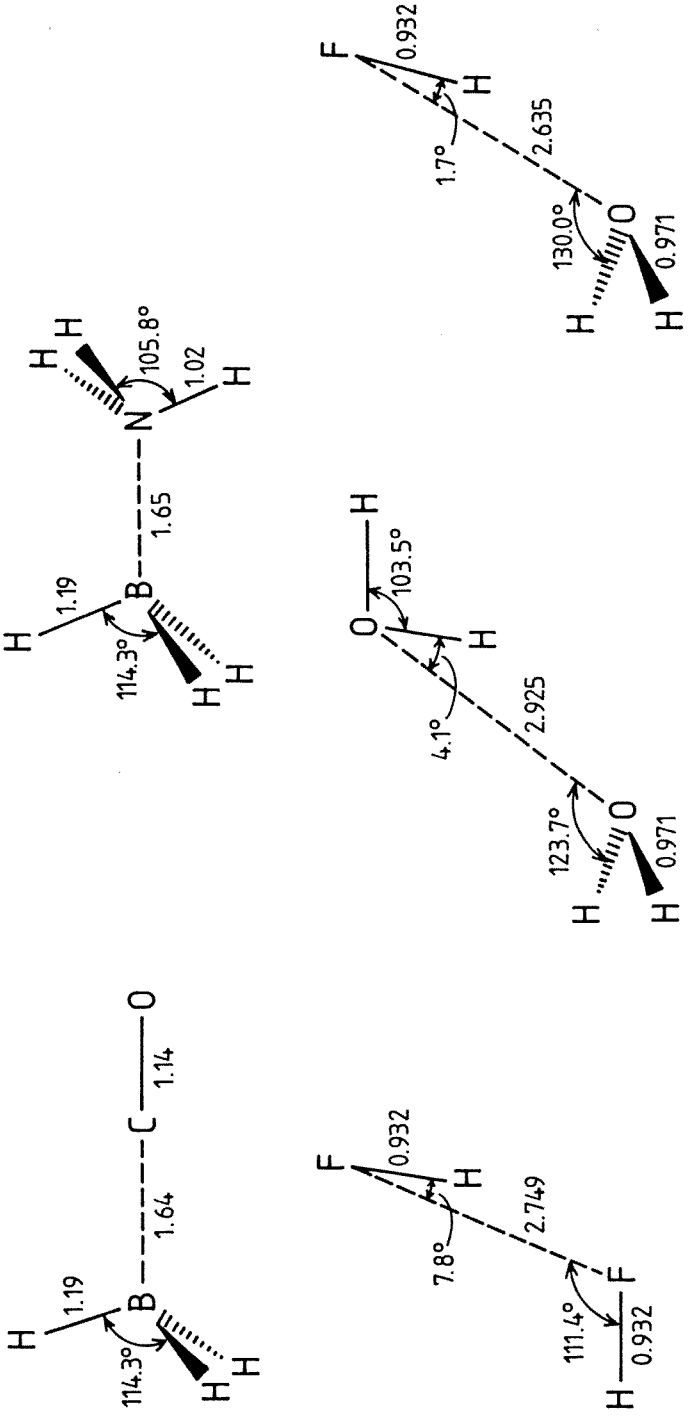

Fig. 1. Equilibrium structures of the strongly bonded EDA complexes and hydrogen bonded systems studied in this work.

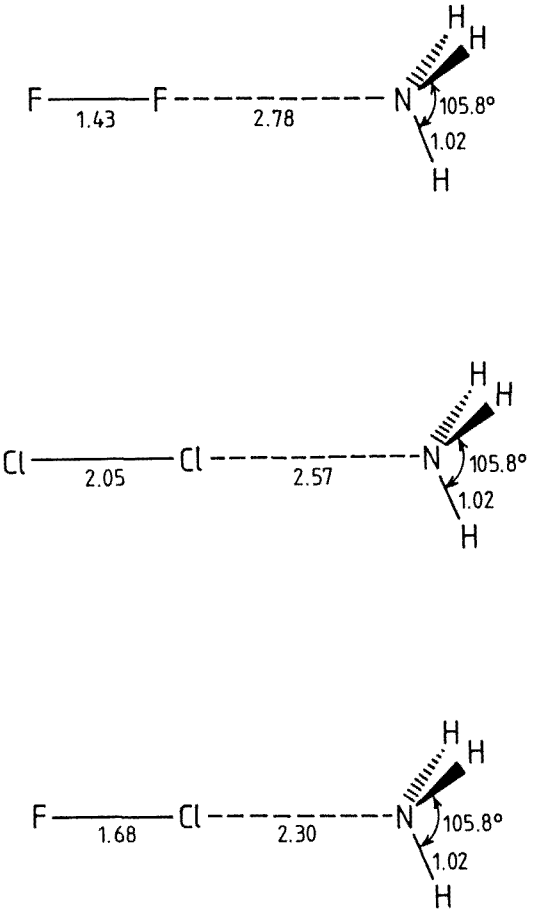

Fig. 2. Equilibrium structures of the weakly bonded EDA complexes studied in this work.

adduct transparent. As in the BH_3CO complex, the bonding is essentially due to a lone pair approaching the "vacant" space in the vicinity of the boron nucleus. The lone pair charge centroid is shifted 0.25271 a.u. away from the nitrogen nucleus and towards the boron nucleus. The electric dipole moment of ammonia increases from 0.6563 a.u. to 1.3257 a.u. during formation of the complex. The changes of the borane subsystem are clear-cut. The charge centroids of the valence geminals are moving away from the boron nucleus, the charge ellipsoids are rotated away from the approaching ammonia subsystem and they expand. The electric dipole moment of borane changes from 0.0 a.u. to 0.7894 a.u. during formation of the complex.

In figs. 5 to 7, we display the intersection between selected charge ellipsoids and the symmetry plane for the hydrogen bonded systems. These figures clearly indicate that the characteristic feature of hydrogen bonding is essentially due to a

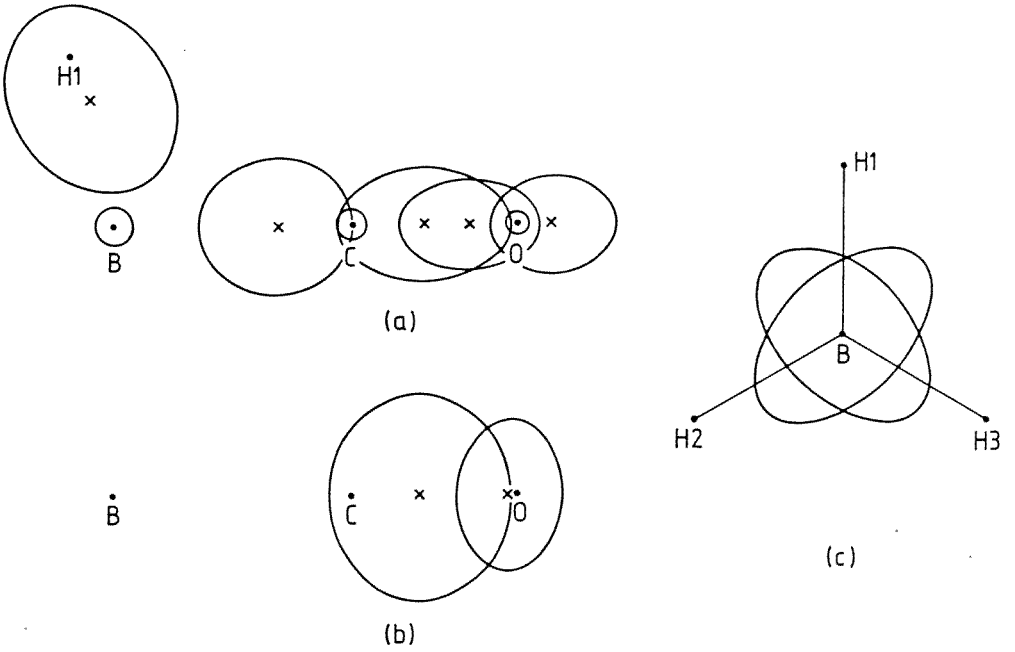

Fig. 3. Intersections between coordinate planes and selected charge ellipsoids of $BH_3 \ldots CO$. In (a), the following ellipsoids are displayed: the core pair ellipsoids of B, a (B–H) bond pair ellipsoid, the core and lone pair ellipsoids of CO, and the two σ-type GVB bond pair ellipsoids of CO. In (b), the intersection between a set of π-type bond pair ellipsoids and a plane containing the longest half-axis of the ellipsoids and the BCO-axis is displayed. The orientation of two π-type ellipsoids with respect to the hydrogen atoms is displayed in (c). The geometry is the equilibrium geometry. Charge centroids are marked with a cross (×) and nuclear positions with a dot (•).

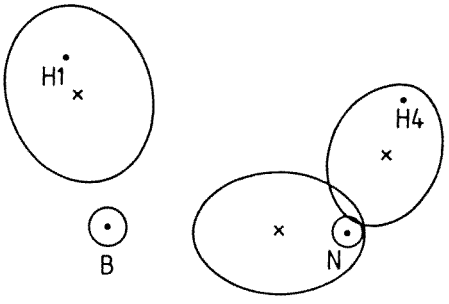

Fig. 4. Intersection between the xy-plane and selected charge ellipsoids of $BH_3 \ldots NH_3$. The nuclei are *rotated to eclipsed configuration*, otherwise the geometry is equal to the equilibrium geometry. Charge centroids are marked with a cross (×) and nuclear positions with a dot (•).

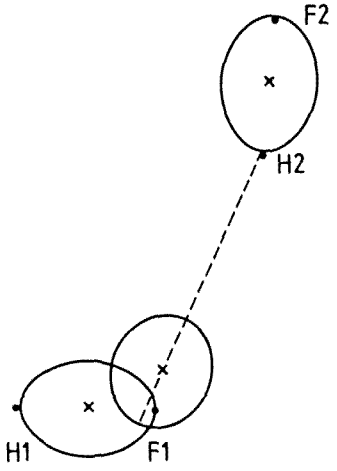

Fig. 5. Intersections between the xy-plane and selected charge ellipsoids of $(HF)_2$. The geometry is the equilibrium geometry as determined in ref. [9]. Charge centroids are marked with a cross (×) and nuclear positions with a dot (•).

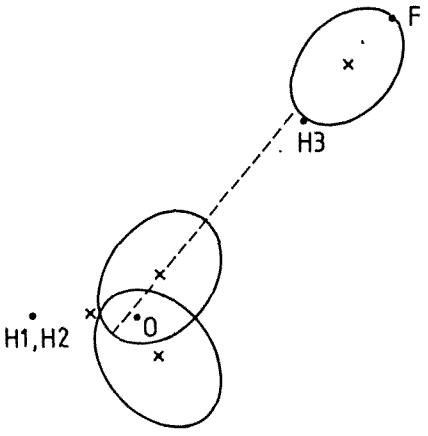

Fig. 6. Intersections between the xy-plane and selected charge ellipsoids of $H_2O \ldots HF$. The geometry is the equilibrium geometry as determined in ref. [9]. Charge centroids are marked with a cross (×) and nuclear positions with a dot (•).

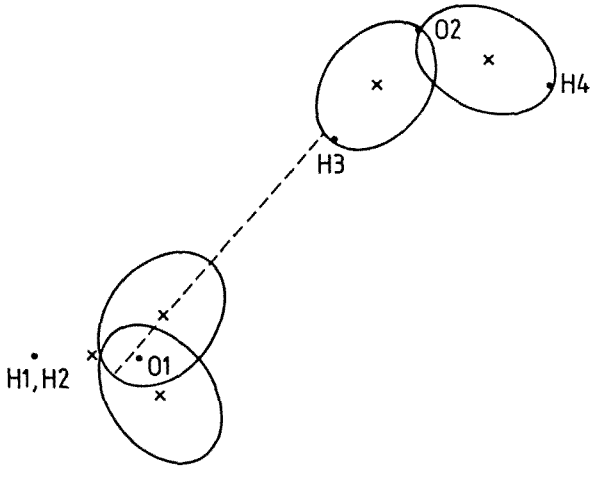

Fig. 7. Intersections between the xy-plane and selected charge ellipsoids of $(H_2O)_2$. The geometry is the equilibrium geometry as determined in ref. [9]. Charge centroids are marked with a cross (×) and nuclear positions with a dot (•).

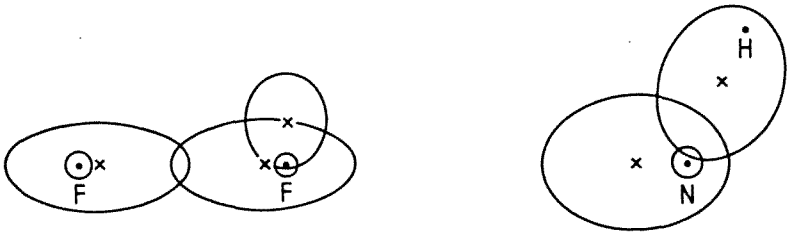

Fig. 8. Intersection between the xy-plane and selected charge ellipsoids of $F_2 \ldots NH_3$. The hydrogen nuclei of NH_3 are rotated to eclipsed configuration with respect to the lone pair ellipsoids of the electron pair accepting fluorine nucleus, otherwise the geometry is equal to the equilibrium geometry as determined in this work. The bond pair of the fluorine molecule is described by two GVB-type orbitals. In the figure, each of the corresponding charge ellipsoids is displayed. Charge centroids are marked with a cross (×) and nuclear positions with a dot (•).

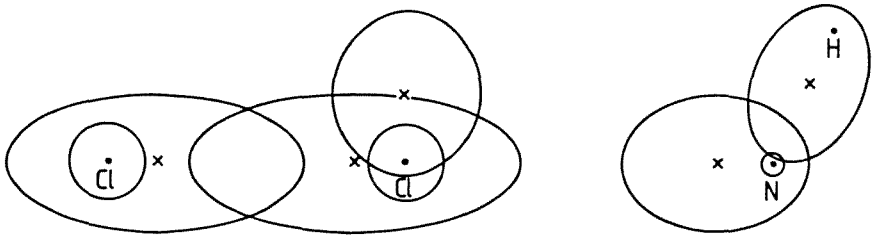

Fig. 9. Intersection between the xy-plane and selected charge ellipsoids of $Cl_2 \ldots NH_3$. The core electron pairs of the chlorine atoms are represented by the smallest spherical surface enclosing the core electron pair ellipsoids. The hydrogen nuclei of NH_3 are rotated to eclipsed configuration with respect to the lone pair ellipsoids of the electron pair accepting chlorine nucleus, otherwise the geometry is equal to the equilibrium geometry as determined in this work. The bond pair of the chlorine molecule is described by two GVB-type orbitals. In the figure, each of the corresponding charge ellipsoids is displayed. Charge centroids are marked with a cross (×) and nuclear positions with a dot (•).

lone pair approaching a hydrogen nucleus. However, the changes of the geminal densities during dimerization are considerably smaller for the hydrogen bonded systems than for the strongly bonded EDA complexes. In $(HF)_2$, the shift of the hydrogen bond pair, i.e. the lone pair approaching the hydrogen nucleus of the acceptor, is only 0.02438 a.u.

In figs. 8 to 10, we display the intersection between a coordinate plane and selected charge ellipsoids of the weakly bonded EDA complexes F_2NH_3, Cl_2NH_3

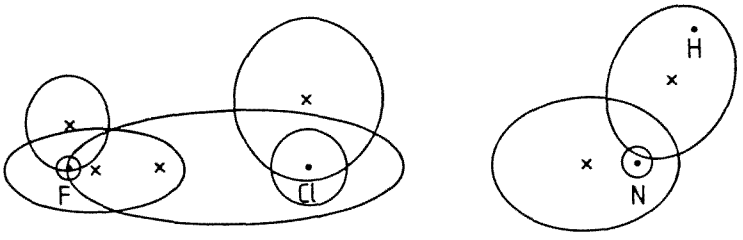

Fig. 10. Intersection between the xy-plane and selected charge ellipsoids of $H_3N \cdot ClF$. The core electron pairs of the chlorine atoms are represented by the smallest spherical surface enclosing the core electron pair ellipsoid. The hydrogen nuclei of NH_3 are rotated to eclipsed configuration with respect to the lone pair ellipsoids of the chlorine nucleus, otherwise the geometry is equal to the equilibrium geometry as determined in this work. The bond pair of the chlorine molecule is described by two GVB-type orbitals. In the figure, each of the corresponding charge ellipsoids is displayed. Charge centroids are marked with a cross (×) and nuclear positions with a dot (•).

and $ClFNH_3$. Also for these systems it makes sense to state that the bonding is essentially due to a lone pair approaching the "vacant" space in the vicinity of the a nucleus of the acceptor system.

4.2. ENERGY DECOMPOSITION

In table 1, we present an energy decomposition of the molecular potential into distortion energies of the subsystems and the components of the interaction energy between the distorted subsystems. Not surprisingly, the dominant terms are the Coulombic interaction and the distortion terms. The "driving force" of the bonding for all complexes is the lone pair of the donor subsystem approaching a nucleus of the acceptor subsystem. This leads to a large Coulombic interaction energy. However, there is a price to be paid. The subsystems are distorted and their internal energies therefore increase. We also notice that the exchange and correlation components of the interaction energy are of the same order of magnitude as the potential.

The similarity between the three classes of complexes becomes most transparent if the components of the energy partitioning are expressed in terms of magnitude of the total interaction energy, i.e. $|E^{(a,d)}|$, as the energy unit. In table 2, the energy components are given as a percentage of this unit, including sign. We notice the remarkable result that the pattern of the rescaled energy components is more or less the same for the EDA complexes and hydrogen bonded systems. For both classes, the dominant binding component is the Coulomb interaction between the distorted subsystems. It represents roughly 80% of the interaction energy. Furthermore, for both classes the donor subsystem is the one which is the most distorted. The

Table 1

Partitioning of the intermolecular potential[1,2]

	EDA complexes		Hydrogen bonded complexes[3]			Weakly bonded EDA complexes		
	BH_3CO	BH_3NH_3	$(HF)_2$	H_2OHF	$(H_2O)_2$	F_2NH_3	Cl_2NH_3	$ClFNH_3$
Δ^a_{dist}	0.199525	0.127733	0.012958	0.027261	0.014313	0.014075	0.107282	0.226300
Δ^d_{dist}	0.269358	0.224824	0.016781	0.040108	0.017894	0.011404	0.064316	0.169496
$\Delta^{a,d}_{coul}$	−0.384396	−0.334706	−0.030072	−0.066942	−0.031570	−0.020037	−0.132945	−0.314220
$\Delta^{a,d}_{exch}$	−0.089974	−0.048307	−0.004843	−0.010349	−0.005618	−0.005880	−0.036604	−0.078593
$\Delta^{a,d}_{corr}$	−0.024281	−0.025852	−0.002270	−0.004590	−0.003246	−0.002170	−0.011406	−0.020139
U	−0.029768	−0.056308	−0.007445	−0.014512	−0.008227	−0.002608	−0.009357	−0.017156

[1] Atomic units.
[2] Equilibrium geometry.
[3] From the work of Røeggen [9].

Table 2

Partitioning of the intermolecular potential using the magnitude of the total interaction energy as energy unit.[1]

	EDA complexes		Hydrogen bonded complexes[2]			Weakly bonded EDA complexes		
	BH_3CO	BH_3NH_3	$(HF)_2$	H_2OHF	$(H_2O)_2$	F_2NH_3	Cl_2NH_3	$ClFNH_3$
Δ^a_{dist}	40.0%	31.2%	34.8%	33.3%	35.4%	50.1%	59.3%	54.8%
Δ^d_{dist}	54.0%	56.0%	45.1%	49.0%	44.3%	40.6%	35.5%	41.0%
$\Delta^{a,d}_{coul}$	−77.1%	−81.9%	−80.9%	−81.8%	−78.1%	−71.3%	−73.5%	−76.1%
$\Delta^{a,d}_{exch}$	−18.0%	−11.8%	−13.0%	−12.6%	−13.9%	−20.9%	−20.2%	−19.0%
$\Delta^{a,d}_{corr}$	−4.9%	−6.3%	−6.1%	−5.6%	−8.0%	−7.8%	−6.3%	−4.9%
U	−6.0%	−13.8%	−20.0%	−17.7%	−20.3%	−9.3%	−5.2%	−4.2%
$\lvert E^{(a,d)}\rvert$[3]	0.498651	0.408865	0.037185	0.081881	0.040434	0.028087	0.180956	0.412952

[1] Equilibrium geometry.
[2] From the work of Røeggen [9].
[3] Atomic units.

distortion energies for the donor and acceptor subsystems are in the range of 44% to 56% and 31% to 40%, respectively. We also notice the stable correlation fraction of the interaction energy, ranging from 4.9% to 8%. What then is the main difference between these two classes of Van der Waals complexes? It is the magnitude of the energy components. This is perfectly understandable. For the hydrogen bonded systems, the bonding electron pair is approaching a small nuclear charge. On the other hand, for the strongly bonded EDA complexes studied in this work, the bonding electron pair is approaching a larger nuclear charge which is only partly screened by the valence electrons. As a result, there will be a larger interaction between these subsystems. For the systems studied in this work, the magnitude of the interaction energy of a strongly bonded EDA complex is an order of magnitude

larger than the corresponding quantity of an hydrogen bonded system. How do the weakly bonded EDA complexes fit into this pattern? The dominant binding component is also in these complexes the Coulombic interaction. However, its relative magnitude is somewhat smaller, i.e. 71% to 76%. The weakly bonded EDA complexes differ from the two other classes by having the acceptor subsystems as the most distorted ones.

As a conclusion of this analysis, we may put forward as a conjecture that the angular arrangement of an EDA or hydrogen bonded complex can very much be decided by looking at a localized representation of the electron density of the donor subsystem and the "vacant" space around the nuclei of the acceptor subsystem.

References

[1] G.C. Maitland, M. Rigby, E.B. Smith and W.A. Wakeham, *Intermolecular Forces* (Oxford University Press, Oxford, 1981).

[2] P. Hobza and R. Zahradnik, Intermolecular complexes. The role of Van der Waals systems, in: *Physical Chemistry* and in the *Biodisciplines* (Elsevier, Amsterdam, 1988).

[3] I. Røeggen, Derivation of an extended geminal model, J. Chem. Phys. 79(1983)5520.

[4] I. Røeggen, Intermolecular potentials calculated by an extended geminal model: Theory, J. Chem. Phys. 85(1986)262.

[5] I. Røeggen and E. Wisløff-Nilssen, Fragment analysis of molecular electronic energies. I. Theory, J. Chem. Phys. 86(1987)2869.

[6] I. Røeggen, Electron correlation described by extended geminal models: The EXGEM4 and EXGEM5 models, Int. J. Quant. Chem. 31(1987)951.

[7] I. Røeggen, Electron correlation described by extended geminal models, J. Chem. Phys. 89(1988)441.

[8] I. Røeggen, Electron correlation described by extended geminal models: The EXGEM7 and EXRHF3 models, Int. J. Quant. Chem. 37(1990)585.

[9] I. Røeggen, An analysis of hydrogen-bonded systems: $(HF)_2$, $(H_2O)_2$ and $H_2O \cdot HF$, Mol. Phys. 70(1990)353.

[10] M.A. Robb, W.J. Haines and I.G. Csizmadia, A theoretical definition of the "size" of electron pairs and its stereochemical implications, J. Amer. Chem. Soc. 95(1973)42.

[11] I.G. Csizmadia, Sizes and shapes of electron pairs, in: *Localization and Delocalization in Quantum Chemistry*, ed. Chalvet et al. (Reidel, Dordrecht, 1975).

[12] S. Huzinaga and C. Arnau, Gaussian-type functions for polyatomic systems. IV, J. Chem. Phys. 53(1970)348.

[13] B. Roos and P. Siegbahn, Polarization functions for first and second row atoms in Gaussian-type MO–SCF calculations, Theor. Chim. Acta (Berl.) 17(1970)199.

[14] L.M.J. Krohn-Batenburg and F.B. van Duijneveldt, The use of a moment-optimized DZP basis set for describing the interaction in the water dimer, J. Mol. Struct. 121(1985)185.

[15] I. Røeggen, An analysis of electron donor–acceptor complexes: $BH_3 \cdot CO$ and $BH_3 \cdot NH_3$, to be submitted to Chem. Phys.

[16] N.H.F. Beebe and J. Linderberg, Simplification in the generation and transformation of two-electron integrals in molecular calculations, Int. J. Quant. Chem. 12(1977)683.

[17] I. Røeggen and E. Wisløff-Nilssen, On the Beebe–Linderberg two-electron integral approximation, Chem. Phys. Lett. 132(1986)154.

[18] J. Breulet and L. Lievin, Comparative theoretical study of the dissociation process of the isoelectronic molecules BH_3CO, CH_2CO, HNCO, CO_2 and BH_3N_2, CH_2N_2, HN_3, N_2O, Theor. Chim. Acta (Berl.) 61(1982)59.